Tropospheric scatter propagation

by J. N. GANNAWAY, DPhil, G3YGF*

Introduction

This article is intended to demonstrate the potential of communications using tropospheric scatter (troposcatter) on the vhf, uhf and microwave bands. The troposcatter propagation mode is regularly used for dx working at vhf, but the predictability of the mode and its potential on the higher frequency bands are not widely appreciated. The nature of troposcatter propagation is explained and an expression for the path loss is given, taking into account the characteristics of the sites at each end. By combining this expression with calculations of the equipment performance at each end of the path, it is possible to predict the signal-to-noise ratio that should be obtained between the two stations under normal conditions, or to estimate the maximum range that can be expected from a given site.

Paths that involve only line-of-sight propagation are not very common, and usually the signals will have been scattered off or diffracted around several obstacles on the way. As the length of the path increases, so does the number of obstructions or the angles through which the signals have to be diffracted. Under these conditions signal levels will decrease very rapidly with distance, and signals arriving by other propagation mechanisms may be stronger. Propagation beyond the horizon can occur by a variety of methods, usually either by atmospheric ducting or by the signals reflecting off an object which is high enough to be visible to both stations. This object can be, for example, an aircraft, an aurora, or an ionization trail from a meteor. However, these phenomena are only very short-lived, and a more permanent mechanism would be desirable. Satellites or moonbounce are more predictable but, apart from the case of geostationary satellites, can only be used for some of the time.

The mechanism of troposcatter

Troposcatter uses the weak, but reliable reflections that can be obtained from the dust particles, clouds, and refractive index variations that occur in the atmosphere in the region 1,000 to 50,000ft asl, and this mechanism can be used for reliable dx working over distances of many hundreds of kilometres. A brief illustration of the structure of the relevant part of the atmosphere is shown in Fig 1. The air density decreases with height, and reaches one third of its sea level value by about 30,000ft. The refractive index of the atmosphere depends on such properties as its temperature, density and—hence—pressure, humidity, or the presence of liquid water, so variations in any of these properties can scatter the signals. The scattering process is more efficient at lower altitudes where the atmosphere is denser, and where turbulence associated with the weather can have marked effects on the signal levels and characteristics.

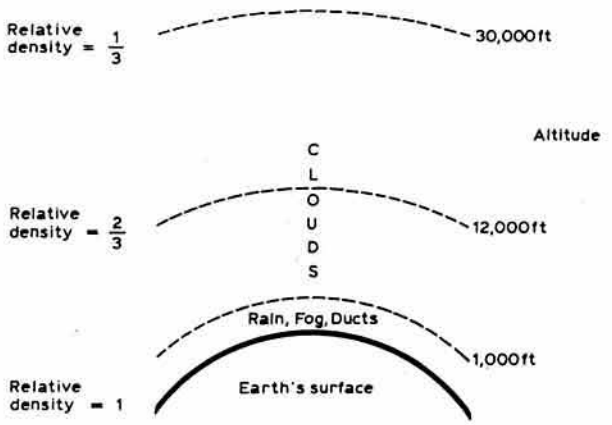

Fig 1. Diagram showing the structure of the lower atmosphere

In practice this mechanism is used by pointing both antennas along the great circle path between the two stations at as low an angle of elevation as possible. The two beams will intersect in a common volume of the atmosphere near the centre of the path, as can be seen from Figs 2 and 3. Propagation will be line-of-sight to the common volume from the transmitter. A very small fraction of the power passing through this volume will then be scattered in all directions by the irregularities in the atmosphere, and some of it will be in the direction of the receiver. This power then propagates by line-of-sight to the receiver. The height of the bottom of this scattering volume will depend on the path length, and to some extent on the horizons of the sites used at each end, but will be typically 2,000ft on a 100km path, and 30,000ft on a 500km path.

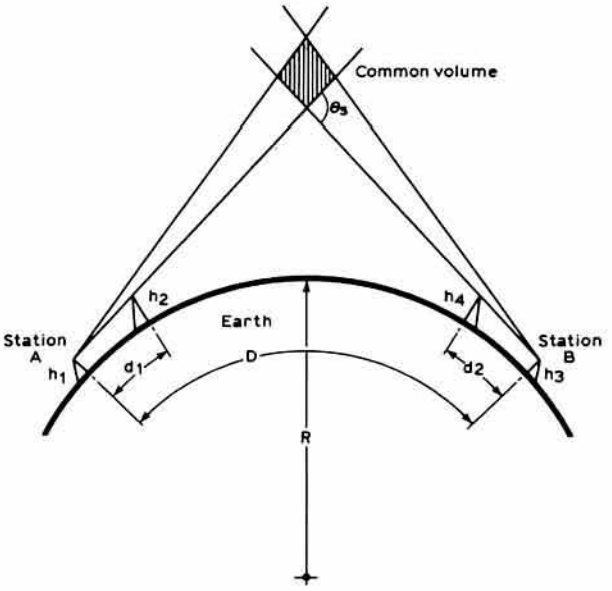

Fig 2. The geometry of a troposcatter path

The loss in the scattering process is usually so large that the equipment is unlikely to have enough spare capability to overcome the extra losses introduced by any additional obstructions in the path. The path loss increases by about 10dB for every degree of horizon angle at each station, and on paths of over 100km by about 9dB for every extra 100km of path length, so the choice of a site with a good horizon is vitally important; it can make a difference of several hundred kilometres to the range obtainable.

Derivation of an expression for the path loss

The angle through which the signal is scattered is an important characteristic of a troposcatter path, as the loss involved increases with angle; the angle involved being usually only a few degrees. The relevant details of a troposcatter path are shown in Fig 2. The heights of each station are h_1 and h_3, and h_2 and h_4 are the heights of the obstructions forming the horizon at each station, at distances of d_1 and d_2 respectively. All heights are with respect to sea level. R is the mean effective radio radius of the earth, 1·33 times the physical radius, 6,371 × 4/3, ie 8,497km, which allows for the amount by which the atmosphere refracts the signals towards the earth's surface under normal conditions. θ_S is the scattering angle which is determined by the path geometry, and consists of three terms: one depending on the overall path length, and two being characteristic of the sites at each end.

*Dept of Engineering Science, Parks Road, Oxford

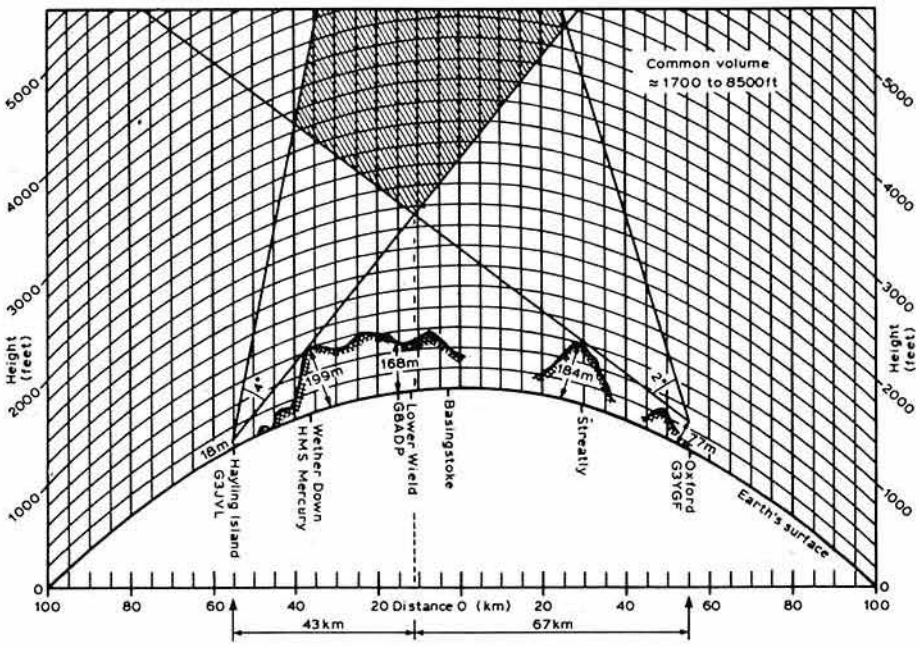

Fig 3. Path profile plot for the Oxford to Hayling Island path

$$\theta_s = \frac{D}{R}\times\frac{180}{\pi} + \underbrace{\left(\frac{h_2-h_1}{d_1} - \frac{d_1}{2R}\right)\times\frac{180}{\pi}}_{\theta_A} + \underbrace{\left(\frac{h_4-h_3}{d_2} - \frac{d_2}{2R}\right)\times\frac{180}{\pi}}_{\theta_B} \quad \text{(degrees)}$$

term in path length — contribution from site A — contribution from site B

The units used for the various distances do not matter, provided that they are the same in each term. It would be convenient to use metres or kilometres throughout. The path loss can now be expressed as the sum of several components:

(1) The free space loss [1]

$$L_{fs} = 32{\cdot}5 + 20\log D + 20\log F \quad \text{(dB, km, MHz)}$$

(2) The loss in the scattering process

$$Ls = 21 + 10\theta_S + 10\log F \quad \text{(dB, degrees, MHz)}$$

This is an empirical expression derived from observed signal levels, and shows the variation of scattering efficiency with frequency and scattering angle. The loss increases by 10dB/° of scattering angle.

These expressions are plotted in Fig 4, which shows the free space loss and the sum of the free space and scatter losses for comparison, indicating that much greater losses are involved in troposcatter, and that they increase very rapidly with distance.

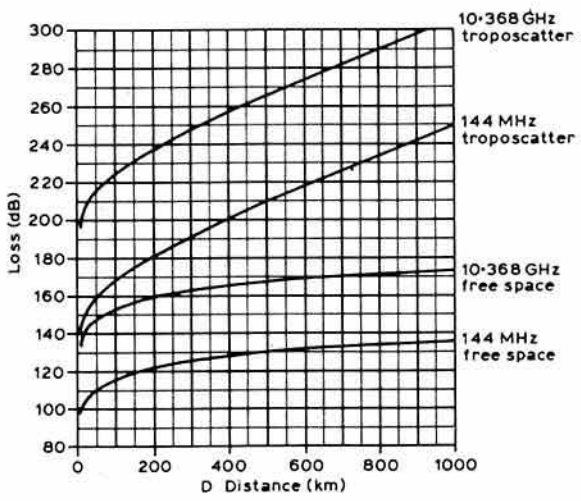

Fig 4. Comparison of troposcatter and free space path losses

(3) The aperture to medium coupling loss [2]

$$L_{am} = 2 + 2\frac{\theta_S}{a} \quad \text{(dB, degrees)}$$

Where a is $\sqrt{\theta_1\theta_2}$, the geometric mean of the two antenna beamwidths. This takes into account the size of the two beams and the way in which they cross in the atmosphere, which affects the efficiency of coupling between them. It implies that there is no point in increasing the size of the antennas above a certain gain on a given path, as the expected increases in gain will not be realized when very high gain antennas are used. This condition occurs when the antenna beamwidths approach the scattering angle, ie a few degrees. This term will be negligible except on the higher frequency bands where antennas with a beamwidth of a few degrees can be realized conveniently, eg a 4ft dish on 10GHz has a 2° beamwidth.

(4) Loss due to variation of the mean radio refractive index of the atmosphere

$$L_n = 0{\cdot}2\,(N-310) \quad \text{(dB)}$$

N is the refractive index expressed in millionths above unity—the nominal value is 1·00031—and will be affected by the climatic conditions mentioned earlier. If N varied by 30 units, this would affect the path loss by 6dB, so it has a significant effect and probably accounts for the seasonal variations referred to later.

Calculation of the path loss

The total troposcatter loss is the sum of all these terms. It is convenient to split it into two parts; one being the basic loss which only depends on the distance and frequency, and the other being the variable losses due to the nature of the sites used and the climatic conditions.

The first part, the troposcatter loss between two stations on a smooth earth [3], is obtained by taking the terms which are either constant or depend on path length or frequency.

$$L = \underbrace{55{\cdot}5 + 20\log D + 30\log F}_{(32{\cdot}5+21+2)} + \underbrace{\frac{D}{R}\times 1{,}800/\pi}_{\text{Path length dependent part of } \theta_S} \quad \text{(dB, km, MHz)}$$

This loss is plotted against distance in Fig 5 (a) and (b) for the frequencies 10,368 and 144MHz. These graphs can be used at other frequencies by adding $30\log\frac{F}{10{,}368}$ or $30\log\frac{F}{144}$ to the value obtained from the appropriate curve. Values of this term for the various amateur bands are given in Table 1. The remaining terms are the variable ones which depend on the sites or propagation conditions and weather, so these should then be added to the loss obtained from the graph:

$$L_V = \underbrace{10\theta_A}_{\text{site A}} + \underbrace{10\theta_B}_{\text{site B}} + \underbrace{\frac{2\theta_S}{a}}_{\text{Parts of } \theta_S \text{ dependent on site A and site B}} - 0{\cdot}2(N-310) \quad \text{(degrees, dB)}$$

Table 1. Corrections to the path loss in Fig 5 for different frequencies

Band	Correction (dB) to be added to the loss given in Fig 5(a) (10,368MHz)	Fig 5(b) (144MHz)
24GHz*	+11	+67
10GHz	−0	+56
5·6GHz	−8	+48
3·4GHz	−15	+41
2·3GHz	−20	+36
1,296MHz	−27	+29
432MHz	−41	+14
144MHz	−56	0
70MHz	−65	−9

*An additional allowance must be made for water vapour absorption on this band

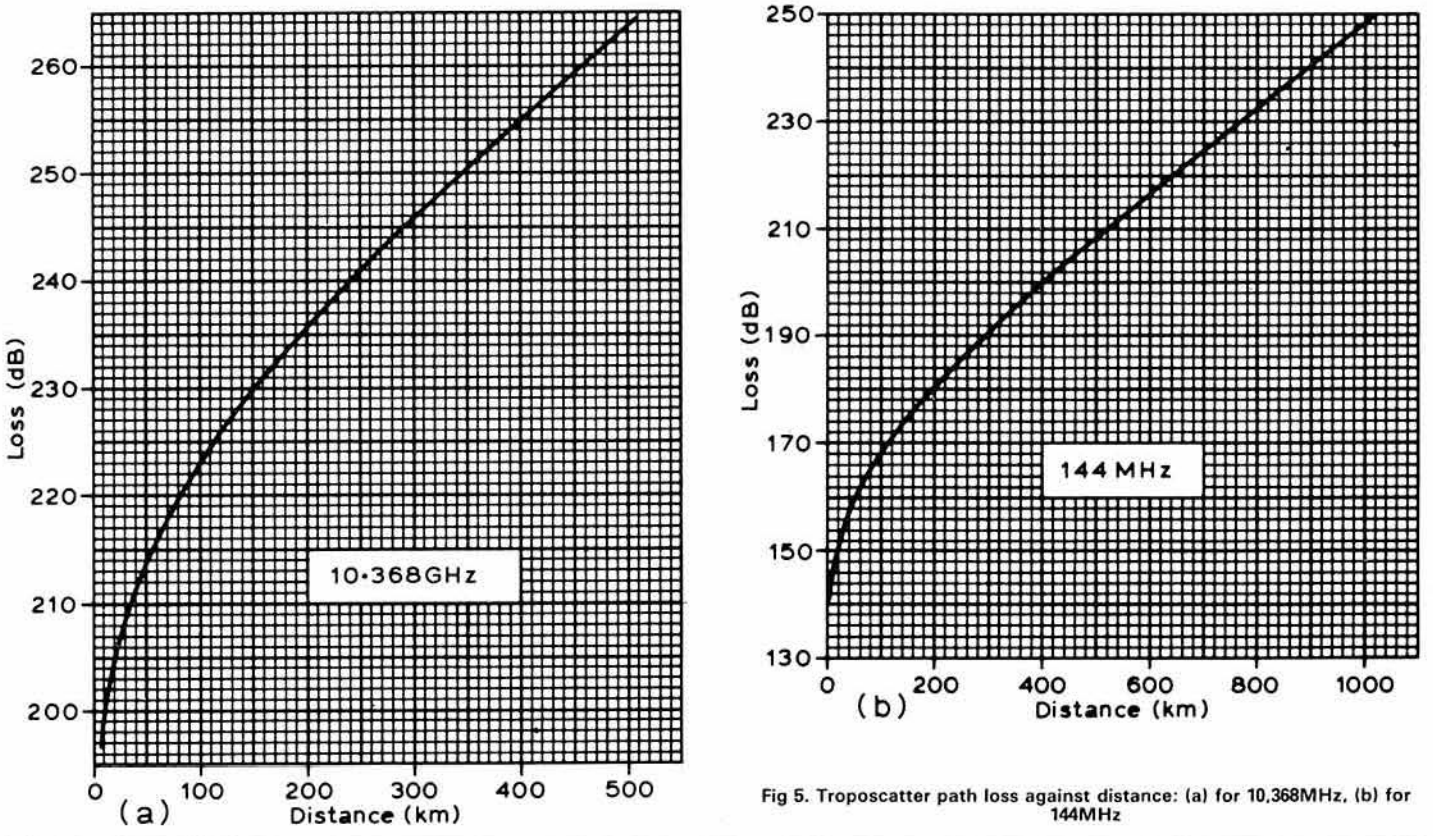

Fig 5. Troposcatter path loss against distance: (a) for 10,368MHz, (b) for 144MHz

For most purposes the total loss can be taken as the loss from the graph plus the contribution from each site. The other two terms will have little effect, and the value of N is not likely to be known accurately.

Once the details of the sites are known, the values of θ_A and θ_B can either be calculated using the expression for θ_S given earlier, or the loss ($10\theta_A$) can be found directly using the graph in Fig 6. In this, d is the distance to the first obstruction, and Δh is the height of the obstruction above the site, see Fig 2.

$$\Delta h = h_{obstruction} - h_{site}$$

The actual height of the site does not appear explicitly in the expressions, only in as much as it determines where the first obstruction is and its height relative to a site. It can be seen from the original expression for θ_S that both the elevation angle that the obstacle presents and its distance from the site are the important parameters in determining the path loss. There is little to be gained by going higher at a site if the object forming the horizon is far away, but significant improvements are possible if the obstacle is very close. A distant horizon is the key feature of a good site which, in simple terms, might be described as a place having a "good view".

It is also very useful to calculate the loss from the site-dependent terms separately, as it provides a means of accurately comparing the merits of various sites and is independent of frequency. Path profile plots [6] should be performed for each direction of interest at each site to find the object causing the horizon and thus the values of d and h. A very good site can give negative values of this loss and so reduce the overall path loss. This loss is typically in the range -5 to $+10$dB.

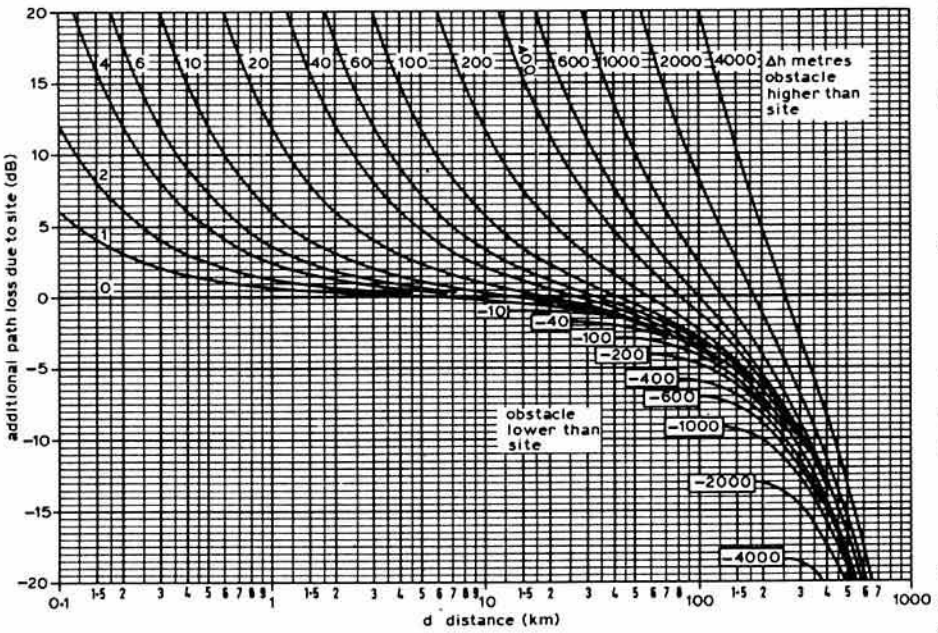

Fig 6. Graph showing the effect of site geography on path loss

Example of path loss calculation

As an example, consider the Oxford–Hayling Island path, a distance of 110km. Taking the distances from the path plot in Fig 3, the site losses are:

$$\theta_A, \text{ Oxford} = 57{\cdot}3\left(\frac{184-77}{26{,}000\text{m}} - \frac{26}{17{,}000\text{km}}\right)$$

$$\theta_A = 0{\cdot}23 - 0{\cdot}09 = 0{\cdot}14^\circ \quad \text{Loss} = 10\theta_A = 1{\cdot}4\text{dB}$$

$$\theta_B, \text{ Hayling Island} = 57{\cdot}3\left(\frac{199-18}{18{,}000\text{m}} - \frac{18}{17{,}000\text{km}}\right)$$

$$\theta_B = 0{\cdot}57 - 0{\cdot}06 = 0{\cdot}51^\circ \quad \text{Loss} = 10\theta_B = 5{\cdot}1\text{dB}$$

The total loss due to the sites is 6·5dB.

The same results can be obtained by using these values of Δh and d in Fig 6.

Site A: $d = 26$km, $\Delta h = 107$m
Site B: $d = 18$km, $\Delta h = 181$m

Next, θ_S is needed to calculate the coupling loss. θ_S is the sum of the horizon angles at each site, plus the term in the total path length, $\frac{57{\cdot}3d}{R}$.

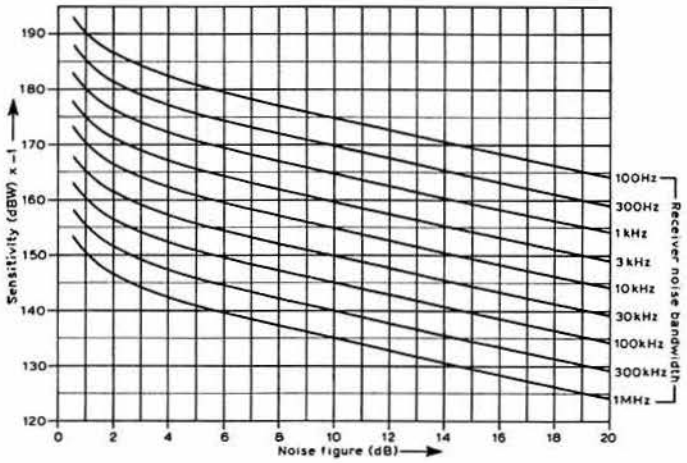

Fig 7. Graph of effective receiver sensitivity as a function of noise figure and bandwidth

$$\theta_S = \underset{\text{Oxford A}}{0{\cdot}14} + \underset{\text{Hayling Is B}}{0{\cdot}51} + \underset{\text{Path length term}}{57{\cdot}3 \times \frac{110\text{km}}{8{,}497\text{km}}} = 1{\cdot}4°$$

Now the coupling loss can be found. The antennas, 2ft and 4ft dishes, have beamwidths of 4° and 2° on 10GHz, so the mean is 2·5°. The coupling loss is then $\frac{2{\cdot}8}{2{\cdot}5}$, approximately 1dB, which is negligible as expected.

The path loss from the graph in Fig 5 for a path of 110km is 244dB at 10GHz, so the total loss is:

Path loss = 224 + 6·5 + 1 = 232dB on 10,368MHz

The path loss on 144MHz can be found in a similar manner. The site losses will be the same, as they are independent of frequency, and the coupling loss will be even smaller since θ_S is the same but the antenna beamwidths are much larger, typically 20 to 30°. The path loss from the graph is 168dB, so the total loss is:

Path loss = 168 + 6·5 + 0 = 175dB on 144MHz

These values are the mean values of loss averaged over a year. There are many factors that will affect this value slightly, and these are discussed later.

Equipment performance

Now that the path losses (pl), are known, the next step is to calculate the capability of the equipment at each end of the path—the path loss capability (plc) [5]. This is the number of decibels of loss that must be inserted between the transmitter and receiver antennas to give a 0dB signal-to-noise ratio in the receiver. The difference between the two terms gives the signal-to-noise ratio to be expected in the receiver: s:n = plc − pl.

The plc can be found for any two sets of equipment, and is the sum of the transmitted effective isotropic radiated power (eirp) and the effective receiver sensitivity (ers): plc = eirp + ers.

The eirp is the sum of the transmitter power in decibels relative to 1W (dBW), and the antenna gain is in decibels relative to an isotropic radiator (dBi), the feeder loss in decibels: eirp = transmitter power (dBW) + antenna gain (dBi) − feeder loss (dB).

Calculation of the ers is slightly more involved. The noise level of the receiver is expressed in decibels below 1W, but as a positive number of decibels. The noise level can be found from the expression for thermal noise, $-10\log(kTB)$, where k is Boltzman's constant, $1{\cdot}38 \times 10^{-23}$ WK^{-1} Hz^{-1}, T is the receiver noise temperature which is related to the more familiar noise figure by the relation $nf = 10\log(1 + \frac{T}{290})$, and B is the receiver bandwidth in hertz. Values for this noise level can be found from the graph in Fig 7 which is for modes such as ssb or cw which have no detector threshold. For a.m. detectors the threshold is 2·6dB, but for fm the situation is more complicated [7], and the threshold increases with modulation index up to about 10dB for wideband fm. These values represent reductions in the receiver's sensitivity. Feeder loss and antenna gain are included as for eirp: ers = receiver noise level (dBW, a positive number of decibels) + antenna gain (dBi) − feeder loss (dB) − threshold (dB).

Examples of plc

The plc will now be calculated for the equipment used on the path mentioned earlier on both 144 and 10,368MHz.

144MHz

G3JVL (transmit)		G3YGF (receive)	
Transmitter 20W	+13dBW	Receiver, nf 5dB, bandwidth 2·5kHz	+166dBW
Feeder loss	−1dB	Feeder loss	0dB
Antenna, 14-el	+14dBi	Threshold (ssb)	0dB
		Antenna, 4-el	+6dBi
	eirp = +26dBW		ers = +172dBW

so plc = eirp + ers = 198dB.

10,368MHz

G3JVL (transmit)		G3YGF (receive)	
Transmitter, 5W	+7dBW	Receiver, nf 8dB, bandwidth 500Hz	+169dBW
Feeder loss	−2dB	Antenna, 4ft dish	+39dBi
Antenna, 2ft dish	+34dBi	Feeder loss	−2dB
		Threshold (cw)	0dB
	eirp = +39dBW		ers = +206dBW

so plc = 245dB.

The path losses calculated earlier are 232dB (10,368MHz), and 175dB (144MHz). The predicted signal-to-noise ratios can now be calculated:

	Predicted value	Observed value
10,368MHz:	245 − 232 = 13dB	10dB
144MHz:	198 − 175 = 23dB	17dB

The 144MHz measurement was only done on one day, so it is likely to be rather inaccurate, but the 10,368MHz measurements were done over a period of many months and show good agreement with the predicted values. The discrepancy is probably due to the seasonal and climatic variations, for which no allowance has been made, although there will always be a few decibels of uncertainty in the equipment parameters, antenna gains etc.

The potential of troposcatter communications

Details of various systems and the range that can be expected between two stations using them are given in Table 2 to illustrate the performance that should be expected under flat conditions from good sites. The loss contributions from the sites are assumed to be zero, and the figures are given for a signal-to-noise ratio of 0dB in a 100Hz bandwidth, representing a weak cw signal. The range obtained when using ssb in a bandwidth of 2kHz, a factor of 13dB larger, will be reduced by about 130km on each band. The equipment is typical of that which might be used for a serious entry in a portable contest. The noise figures given may seem rather high, but are those of the overall system, which may be significantly higher than those of the preamplifiers on their own.

Table 2. Range obtainable by troposcatter propagation on various amateur bands

(100Hz bandwidth receiver)

Freq (MHz)	Path loss (dB)	Range (km)	Equipment	Antenna gain
144	240	870	100W, 3dB nf, 2× 16-el Yagi	18dBi
432	247	790	100W, 3dB nf, 2× 25-el loop Yagi	22dBi
1,296	258	760	100W, 3dB nf, 4× 25-el loop Yagi	24dBi
2,304	262	720	50W, 3dB nf, 6ft dish	31dBi
10,368	234	240	100mW, 10dB nf, 4ft dish	39dBi
10,368	254	440	1W, 3dB nf, 4ft dish	39dBi

Table 3 gives the troposcatter range between two systems which are capable of moonbounce communication to illustrate the relative magnitudes of the problems involved. For distances approaching 1,000km, the challenge represented by the two modes of communication can be seen to be comparable. These tables also show that the range attainable by troposcatter need not, in theory, vary much with frequency. In practice, however, physically smaller antennas tend to be used on the higher frequencies, and it is also harder to generate comparable powers on the higher bands. In view of the rapid advances being made in receiver and transmitter technology, however, the potential of the microwave bands for longer distance communication should not be ignored.

Table 3. Troposcatter range of equipment capable of moonbounce operation

Freq (MHz)	EME path loss (dB)	Tropo range (km)	Equipment	Antenna gain
144	252	990	500W, 3dB nf, 100Hz, 4× 16-el Yagi	21dBi
432	262	940	500W, 3dB nf, 100Hz, 20ft dish	26dBi
1,296	271	890	500W, 3dB nf, 500Hz, 16ft dish	34dBi
2,304	276	860	100W, 3dB nf, 500Hz, 16ft dish	40dBi
10,368	289	790	50W, 3dB nf, 1kHz, 12ft dish	50dBi

Oscilloscope traces showing rapid fading on troposcatter signals received from G3JVL on 10,368MHz over a 110km path in March 1979

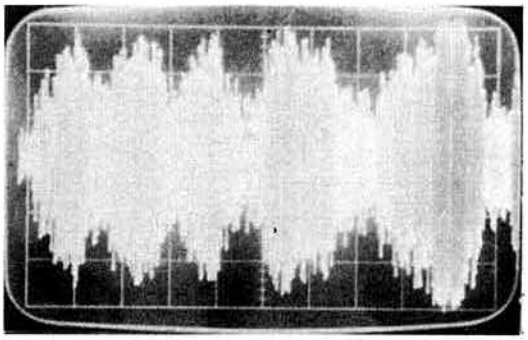

Photo 1. Continuous carrier, 50ms/cm, showing fading at around 10Hz

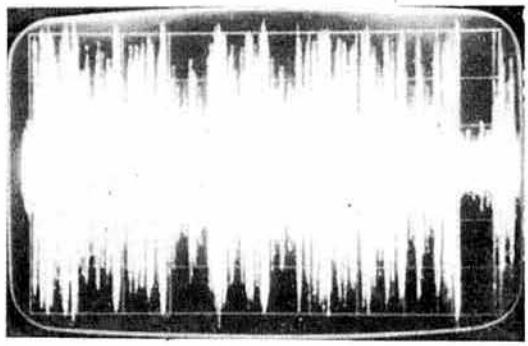

Photo 3. Continuous carrier showing fading on a longer time scale, 0·6s/cm

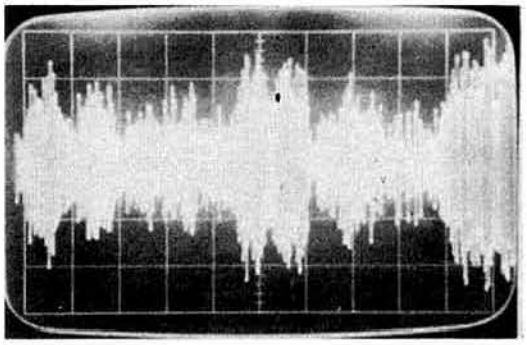

Photo 2. Continuous carrier, 50ms/cm, showing more random fading

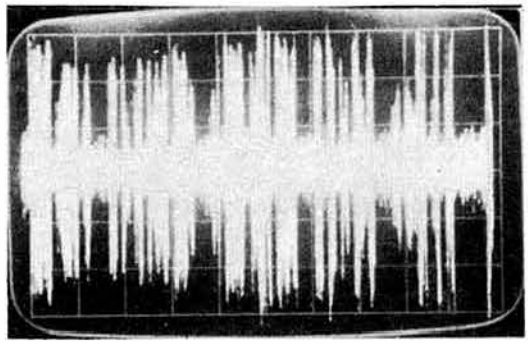

Photo 4. Morse code from G3JVL showing occasional deep fading, 0·6s/cm

Characteristics of troposcatter signals

Several different types of fading are experienced on troposcatter signals [4]. The effects are more severe at high frequencies, so are easier to observe and describe. At 10GHz the note of the carrier can appear quite rough, being modulated by the scattering process at frequencies up to about 50Hz. An example of this rapid fading is shown in Photos 1 and 2, which are oscilloscope photographs of a continuous carrier received over a 110km path from G3JVL to G3YGF, showing both the depth of the fading and range of frequencies over which it occurs. At times it produces a waveform that resembles 100 per cent amplitude modulation. Photo 3 shows the fading on a longer time scale, and the occasional very deep fades can corrupt cw as shown in Photo 4, where in the V of G3JVL the dash has been broken up into two dots.

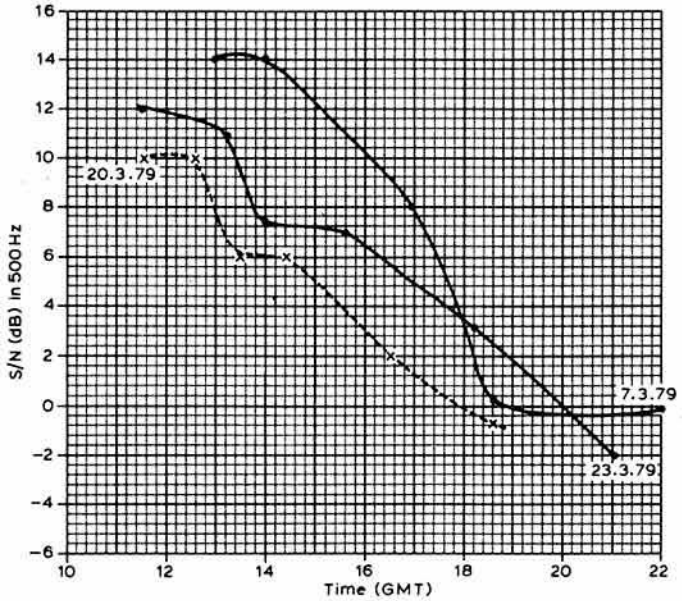

Fig 8. Plots of signal strength against time showing diurnal variations

There is also fading over a period of minutes and, in the longer term, signals tend to show a diurnal variation of about ±5dB, often peaking in the afternoon when atmospheric turbulence caused by convection currents from the warm ground is at a maximum. Plots of signal level showing this effect are given in Fig 8. There is also an annual variation of similar amplitude, with signals peaking in the summer, and being at a minimum in the winter. The daily and annual variations are probably the result of corresponding variations in the average value of N over the path. These fading effects will all exist at lower frequencies, but the rates and depth of the short-term fading will be correspondingly slower, and can be seen as the slow fading on vhf dx signals which has a period of several minutes.

The rapid fading is caused by the signal being scattered from various regions of air, each of which may be in turbulent motion, and moving relative to each other. This motion can cause both frequency and amplitude modulation of the signals. Frequency modulation results from the signals being scattered from air masses that are moving at different speeds, so there will be random doppler shifts on the signals. At 10GHz a speed of 30mph will produce a shift of about 500Hz, and this effect can spread the energy of the carrier out over 1kHz or more; heavy rainstorms producing a sound rather similar to an auroral signal. This effect will also scale with frequency and so will be far less noticeable at vhf. These storms can also increase the signal levels by around 10–20dB, as the raindrops scatter the signal more effectively. Amplitude modulation results from variations in the scattering efficiency or interference effects between signals arriving by different paths.

Several enhancements of 10–15dB on 10GHz have occurred at the same time as big lifts on the vhf bands, eg on 10 November 1978 and 3 October 1980, when the note was T9 and very good quality ssb was obtained, showing that the clean signal that was enhanced by the ducting had swamped the normal, rough troposcatter one.

Conclusion

This method of calculating troposcatter path losses has given predictions of signal levels that have been shown to be accurate to within a few decibels over a number of paths on 144MHz and 10GHz from 100 to 500km long, when used in conjunction with the calculations of the path loss capability of the equipment.

(Continued on page 717)

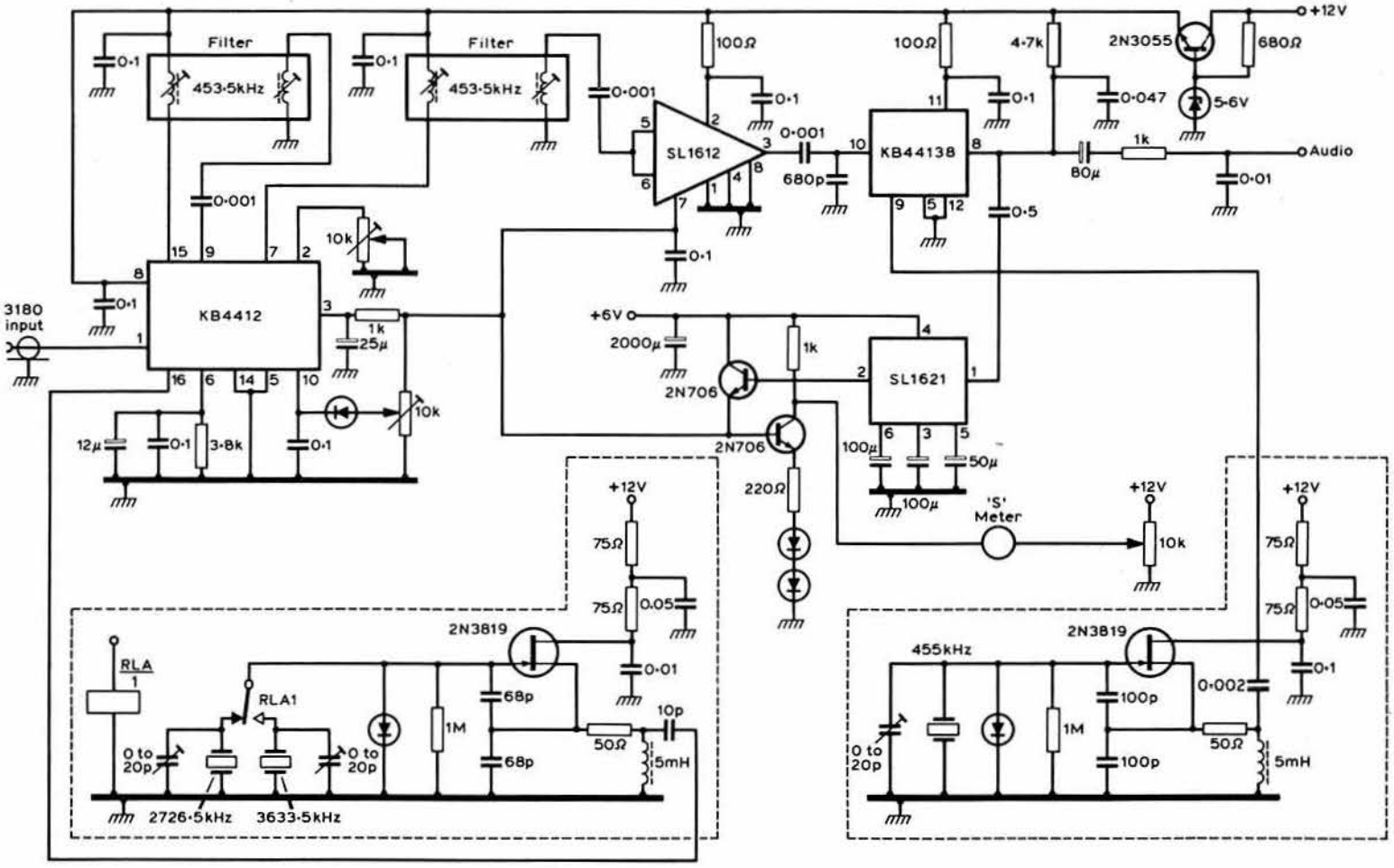

Fig 2. Circuit diagram of the Q5er

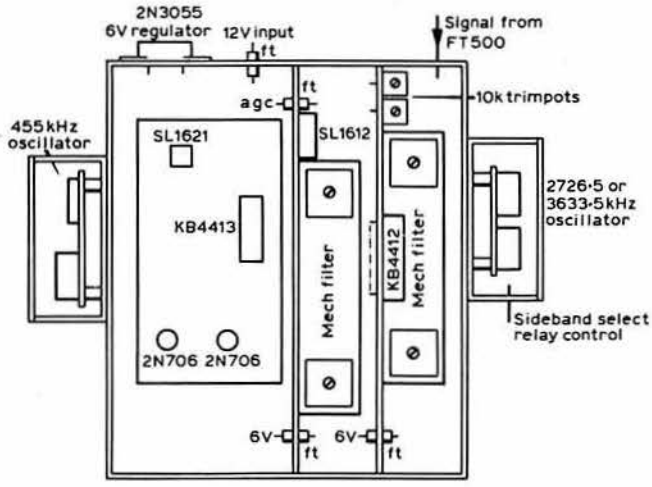

Fig 3. Plan of layout arrangement. The screens are cut from copper-clad glass-fibre board. The filters are soldered on to the copper foil of the screen

The power supply and audio amplifier are straightforward and not shown in the circuit diagram.

There is no reason why this receiver should not be used with any transceiver having a 3,180kHz i.f., or indeed with a 9MHz i.f. and different crystals in the first oscillator. To find the correct frequency for the oscillators add the *centre frequency* of the mechanical filter to the centre frequency of the receiver's filter for one crystal; and subtract the frequency of the mechanical filter from the frequency of the receiver's filter for the other crystal. Note that the centre frequency of the MFL455 is 453·5. □

Tropospheric scatter propagation

(Continued from page 714)

It enables the merits of various sites to be compared more scientifically, and an estimate to be given of the distances that should be workable under flat conditions. It has also demonstrated the potential of narrowband modes on 10GHz and revealed several interesting propagation effects that can be investigated. The papers in the references will provide more background information on the subject, and are quite light reading.

Acknowledgements

The author would like to thank G3JVL, G3RPE and G3WDG for their advice during the production of this article.

References

[1] "Microwaves", *Radio Communication* May 1978.
[2] "Theory of radio transmission by tropospheric scattering using very narrow beams", Booker and De Bettencourt. Proc IRE, March 1955, p281.
[3] "Simple methods for designing troposcatter circuits", Leang Yeh. IRE Transac comms systems, Sept 1960, p193.
[4] "Results of propagation tests at 505 and 4,090MHz on beyond the horizon paths", Bullingdon, Inkster and Durkee. Proc IRE, Oct 1955, p1306.
[5] "Microwaves", *Radio Communication* March 1978.
[6] "Microwave path checking", B. Chambers, G8AGN. *Radio Communication* March 1978.
[7] "On theoretical signal to noise ratios in fm receivers", D. Middleton. *J Appl Phys* April 1949, Vol 20, pp334-51). □